Dopant-Induced Nanoscale Electronic Inhomogeneities in $Ca_{2-x}Sr_xRuO_4$

Jiandi Zhang,[1] Ismail,[2] R. G. Moore,[2] S.-C. Wang,[3] H. Ding,[3] R. Jin,[4] D. Mandrus,[4,2] and E. W. Plummer[2,4]

[1]*Department of Physics, Florida International University, Miami, Florida 33199, USA*
[2]*Department of Physics and Astronomy, University of Tennessee, Knoxville, Tennessee 37996, USA*
[3]*Department of Physics, Boston College, Chestnut Hill, Massachusetts 02467, USA*
[4]*Condensed Matter Sciences Division, Oak Ridge National Laboratory, Oak Ridge, Tennessee 37831, USA*

(Received 31 August 2005; published 14 February 2006)

$Ca_{2-x}Sr_xRuO_4$ single crystals with $0.1 \leq x \leq 2.0$ have been studied systematically using scanning tunneling microscopy (STM) and spectroscopy, low-energy electron diffraction, and angle resolved photoelectron spectroscopy (ARPES). In contrast with the well-ordered lattice structure, the local density of states at the surface clearly shows a strong doping dependent nanoscale electronic inhomogeneity, regardless of the fact of isovalent substitution. Remarkably, the surface electronic roughness measured by STM and the inverse spectral weight of quasiparticle states determined by ARPES are found to vary with x in the same manner as the bulk in-plane residual resistivity, following the Nordheim rule. For the first time, the surface measurements—especially those with STM—are shown to be in good agreement with the bulk transport results, all clearly indicating a doping-induced electronic disorder in the system.

DOI: 10.1103/PhysRevLett.96.066401 PACS numbers: 74.70.Pq, 71.27.+a, 72.10.Fk, 74.25.Jb

Chemically doping a material has been an effective way to explore new emergent phenomena. Striking examples include high-T_c superconductivity in cuprates, ''colossal'' magnetoresistance in manganites, and ferromagnetism in diluted magnetic semiconductors. However, many recent studies have overwhelmingly demonstrated that doping also triggers spatial electronic inhomogeneities in a wide variety of complex electronic materials, even in high-quality single crystals [1]. Nanoscale electronic inhomogeneity occurs between antiferromagnetic insulating and superconducting or metallic states in cuprates [2]. Microscopic to mesoscopic phase separation arises from ferromagnetic metallic and antiferromagnetic insulating phases in manganites [3]. In heavy-fermion compounds [4], inhomogeneous ground states are described as ''electronic Griffiths phases.'' Even in organic crystals such as κ-(BEDT-TTF)^2X [5], electronic phase separation consisting of the metallic and insulating domains appears near the first-order Mott transition. Unraveling the origin and role of inherent inhomogeneity has been a crucial issue toward the understanding of the emergent phenomena in correlated electron materials.

It is generally believed that the coexistence of competing nearly degenerate states in a correlated electron system is conspired by several simultaneously active degrees of freedom: charge, lattice, orbital, and spin. Varying the doping level or composition is expected to influence the balance of these competing states, and thus the inhomogeneity. At present, there is no systematic study of the evolution of inhomogeneous states with doping in a prototype system. In both cuprates [2,6–9] and manganites [3,10,11], chemical dopants play the dual roles: one providing charge carriers and the other introducing local crystalline disorder. While many believe that the doped charges play an important role in the formation of inhomogeneities, emerging evidence indicates that doping-induced random disorder may be crucial as well [12,13]. Whether the inhomogeneity is caused by doped charge carriers or by doping-induced disorder is yet to be resolved.

To gain insight into these unsolved issues, we have used a combination of complementary techniques (LEED, STM, and ARPES) to systematically explore the doping dependence of local electronic inhomogeneity in a prototype transition-metal oxide: $Ca_{2-x}Sr_xRuO_4$. There are three main reasons to choose $Ca_{2-x}Sr_xRuO_4$. First, it is a layered perovskite system thus amenable to obtain an ideal surface by cleaving a single crystal without changing the composition. Second, the *isovalent* substitution between Ca^{2+} and Sr^{2+} introduces only the cation random disorder to the system, thus avoiding charge carrier doping [14]. Last but not least, it is the only-known copper-free transition-metal oxide where the evolution from antiferromagnetism to superconductivity has been explored [14–16]. The phase diagram of $Ca_{2-x}Sr_xRuO_4$ contains rich and exotic behavior attributable to numerous and nearly degenerate structural, electronic, and magnetic instabilities.

STM and ARPES have played a momentous role in the understanding of microscopic electronic properties in many correlated electron systems [6–11,17–25]. In particular, both topographic and spectroscopic images on local density of states (LDOS) with STM have uncovered remarkable electronic inhomogeneities and their possible correlation with local impurity or dopant atom distributions in cuprates [6–9] and manganites [10,11]. However, one vital unsettled issue remains: As a surface-sensitive technique similar to ARPES, can STM probe bulk intrinsic properties by measuring at a surface? In this Letter, we demonstrate that, for the first time, the results measured by these techniques are in good agreement with the bulk transport properties.

High-quality $Ca_{2-x}Sr_xRuO_4$ single crystals used in this study were grown by the floating-zone technique [26] and their bulk properties were well characterized. Both LEED and STM experiments were performed in an ultrahigh vacuum (UHV) system equipped with Omicron LEED optics and a variable temperature STM. While the ARPES measurements were carried out in a separate chamber also equipped LEED optics for confirming the surface quality. $Ca_{2-x}Sr_xRuO_4$ crystals were mounted on the sample plates with conducting silver epoxy and a small metal post was glued on top. The crystal was cleaved by knocking off the post in UHV, producing a flat, shiny (001) surface that yielded a sharp LEED pattern. The surfaces of $Ca_{2-x}Sr_xRuO_4$ for both LEED and STM measurements were acquired by cleaving *in situ* at room temperature (RT) and in a vacuum with the pressure of 1×10^{-10} Torr. Samples for ARPES experiments were cleaved *in situ* and measured at $T = 40$ K in a vacuum better than 8×10^{-11} Torr. We did not observe any obvious difference in surface structure cleaved at different temperatures. All the STM images and spectra were obtained with tungsten tips. Each of the images contains 512×512 pixels and each of local tunneling spectra, i.e., the tunneling current as a function of bias voltage $I(V)$ at a fixed position, have 200 data points. ARPES experiments were performed at the Synchrotron Radiation Center, Wisconsin, using the undulator beam lines (U1 NIM and PGM) at different photon energies (10 to 32 eV). A Scienta analyzer capable of multiangle detection is used with energy resolution of 15 meV, and momentum resolution of 0.02 $Å^{-1}$. The photon energies used were either 22 eV for the samples with $x = 0.3$, 1.0, 1.5, and 1.9 or 32 eV for samples with $x = 0.5$ and 2.0. Samples for all measurements are stable and show no sign of degradation during a typical measurement period of 12 hours after cleaving.

Figure 1 presents characteristic LEED images of a freshly RT cleaved $Ca_{2-x}Sr_xRuO_4$ with $x = 0.1$ (a), 0.5 (b), and 2.0 (c). The sharpness of these images clearly indicates that the surfaces of these samples have a well-ordered lattice structure. Along with the integer spots associated with undistorted bulk cubic perovskite structure [15], faint spots appearing in the middle of four bright integer spots are also observed from all samples. These faint diffraction spots are the result of the in-plane rotational distortion of RuO_6 octahedra [27], For the samples with $x = 0.1$ and 0.5, the LEED patterns show that the surface has a (1×1) structure as compared with the bulk, indicating that the rotational distortion occurs both at the surface and in the bulk. In the case of Sr_2RuO_4 ($x = 2.0$), the appearance of faint spots is due to a surface reconstruction [27]. Bulk Sr_2RuO_4 has a tetragonal structure without the rotational distortion [15].

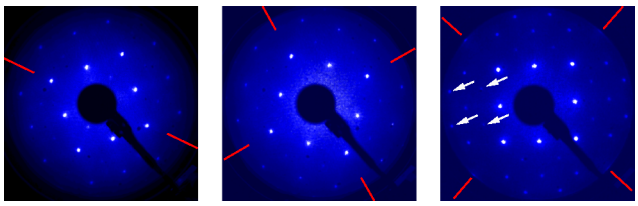

FIG. 1 (color online). LEED patterns from the freshly cleaved (001) surfaces of $Ca_{2-x}Sr_xRuO_4$ at the Sr-doping level (x from left to right) of 0.1, 0.5, and 2.0, taken at the beam energy of 139, 129, and 137 eV, respectively. The arrows mark the faint fractional spots, and the solid lines on which the fractional spots are extinct indicate the surface projections of the glide planes [27].

To obtain information about the local structural and electronic properties, we have performed *in situ* STM measurements at the same cleaved surfaces of $Ca_{2-x}Sr_xRuO_4$ as those used for the LEED experiment. Large scale STM images from all cleaved surfaces show very large terraces up to μm size with step heights of integral multiples of the half-unit cell of $Ca_{2-x}Sr_xRuO_4$ (~6.4 Å), corroborating that the crystals cleave between RuO_6 layers and the surface is terminated with the Ca/Sr-O layer for this system. However, high-resolution images clearly demonstrate a strong doping dependence of surface corrugation, in sharp contrast to the LEED images. Figure 2 shows typical atomically resolved images of $Ca_{2-x}Sr_xRuO_4$ with $x = 0.1$ (a), 1.0 (b), and 2.0 (c). For undoped Sr_2RuO_4 ($x = 2.0$), the STM image shown in Fig. 2(c) exhibits a homogeneous surface structure with regular square atomic lattices. However, superimposed on the ordered lattice matrix, random nanoscale corrugations apparent with the bright (high) and dark (low) regions are seen in the STM images of $Ca_{1.9}Sr_{0.1}RuO_4$ and $CaSrRuO_4$ as shown in Figs. 2(a)–2(c). We have examined many surface areas with different image sizes for samples with different doping concentrations. We found that such disor-

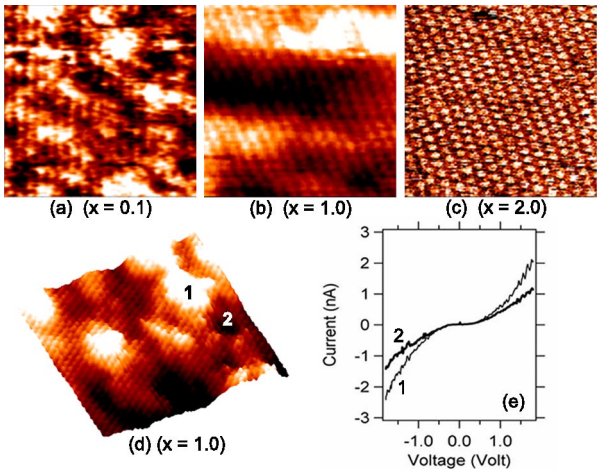

FIG. 2 (color online). 10 nm $\times$ 10 nm STM topography images of the (001) surfaces of $Ca_{2-x}Sr_xRuO_4$ with $x =$ (a) 0.1, (b) 1.0, and (c) 2.0, as well as (d) a 3D view and (e) the averaged STS $I(V)$ curves taken at the two contrast areas on the surface of $CaSrRuO_4$ [marked as "1" for bright area and "2" for dark area in (d) and (e)]. The data were taken at RT, a sample bias $V_s = 1.6$ V, a tunneling current $I_t = 0.5$ nA, and in constant-current mode.

dered nanoscale corrugations are evidently associated with the Ca/Sr-cation random mixing in the system and reaches a maximum in $CaSrRuO_4$. To ensure that changes in the local density of states causes the random corrugations, we have simultaneously performed tunneling spectroscopy and topography measurements. Corresponding to the drastic corrugation image at the surface of $x = 1.0$ sample [Fig. 2(d)], the averaged $I(V)$ curve [shown in Fig. 2(e)] taken in the "bright" area is different from that in the "dark" area, indicating an inherent electronic inhomogeneity.

In order to assess the correlation between the local electronic roughness and the dopant-induced random disorder, we have carried out a surface corrugation analysis of the topographic images of $Ca_{2-x}Sr_xRuO_4$ taken in the same tunneling condition. Figure 3(a) shows the result of the doping dependence of root-mean-square (rms) corrugation which is defined as

$$\langle \mathrm{rms} \rangle = \sqrt{\frac{1}{N}\sum_{j=1}^{N}(Z_j - Z)^2}, \qquad Z = \frac{1}{N}\sum_{j=1}^{N} Z_j, \quad (1)$$

where z_j is the image height at the jth position on the surface, and N is the total acquired data points or pixels in an image ($N = 512 \times 512$). Remarkably, the doping (x) dependence of the electronic roughness coincides with that of the in-plane residual resistivity $\rho_{ab}(0)$ [14]. Both obey the Nordheim rule [28,29]: $\langle \mathrm{rms} \rangle$ and $\rho_{ab}(0) \propto x(2 - x)$ as represented by the solid curve in Fig. 3(a). This implies that the randomness, intrinsic to the cation substitution, is responsible for the observed electronic inhomogeneity and the finite residual resistivity. While the imaged electronic inhomogeneity by STM reflects the different electronic densities of states at nanoscale, the residual resistivity measures the carrier scattering by the random potentials raised by the local inhomogeneous electronic states. The similar doping dependence of surface electronic roughness and bulk residual resistivity demonstrates, for the first time, the surface properties measured with STM do reflect the bulk properties in these layered compounds.

The existence of a nanoscale inhomogeneity will have important consequences on low-energy single-electron excitations such as the quasiparticle (QP) spectral weight (Z_{QP}) [30,31] that are accessible by macroscopic measurements such as ARPES. ARPES can be used to determine the strength of the coherent excitations as a function of momentum and energy. By studying the doping dependence of QP excitations in $Ca_{2-x}Sr_xRuO_4$ with ARPES, we find that the spectral line shape (including spectral weight and linewidth) changes drastically as x varies. Figure 4 displays the energy distribution curves (EDCs) taken in the vicinity of the Fermi surface (FS) along the Γ-M and Γ-X directions, respectively. The observed feature at the Fermi energy (E_F) shown in Fig. 4 is the QP excitations from one of the three t_{2g} bands with d_{xz}/d_{yz} orbital character, giving rise to the electronlike β FS centered at the Γ point [32,33]. It appears as a sharp coherent peak in both directions in Sr_2RuO_4 ($x = 2.0$) but significantly reduces its spectral weight (reduced intensity and increased linewidth) as x decreases down to 1.0. For smaller x (for example, $x = 0.5$), the coherent peak at E_F regains some spectral strength. It is clear that the coherent peak exhibits its minimum intensity at the middle of the doping range ($x = 1.0$). As has been reported recently [33], no major electron transfer among the three t_{2g} bands has been observed in this system. Therefore, an obvious mechanism for the reduction of coherent QP spectral weight is the incoherent scattering due to the doping-induced random disorder.

If the disorder-driven mechanism is responsible for the change of the QP spectra weight, one would expect a further increase of the QP intensity when $x < 0.5$. Surprisingly, the spectral weight of $Ca_{1.7}Sr_{0.3}RuO_4$ ($x = 0.3$) decreases compared with that for $x = 0.5$ (see Fig. 4). To understand this unexpected change, one must realize that $Ca_{1.7}Sr_{0.3}RuO_4$ ($x = 0.3$) is in the vicinity of the Mott insulator ($x < 0.2$) and quantum critical point ($x_c = 0.5$). Its QP spectral weight must thus be affected by strong magnetic fluctuations and Mott-driven localization [14], in addition to the disorder effect. The decrease of its QP

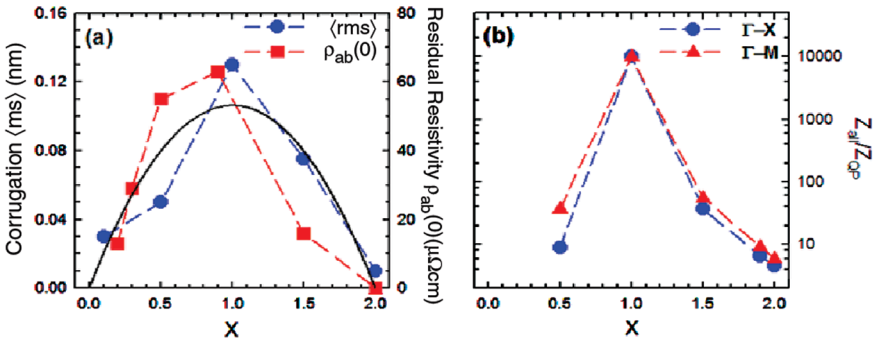

FIG. 3 (color online). (a) The surface electronic corrugation $\langle \mathrm{rms} \rangle$(roughness) of $Ca_{2-x}Sr_xRuO_4$ at RT measured by STM topography images as a function of doping (x), as compared with the in-plane residual resistivity $\rho_{ab}(0)$ from Ref. [14]. The solid curve represents a fit of $\langle \mathrm{rms} \rangle$ to the Nordheim rule; (b) The inverse ratio of the ARPES QP to total excitation spectral weight ($Z_{\mathrm{all}}/Z_{\mathrm{QP}}$) of $Ca_{2-x}Sr_xRuO_4$ ($x \geq x_c$) taken at the k_F of the β FS along both the Γ-X and Γ-M directions (see Fig. 4).

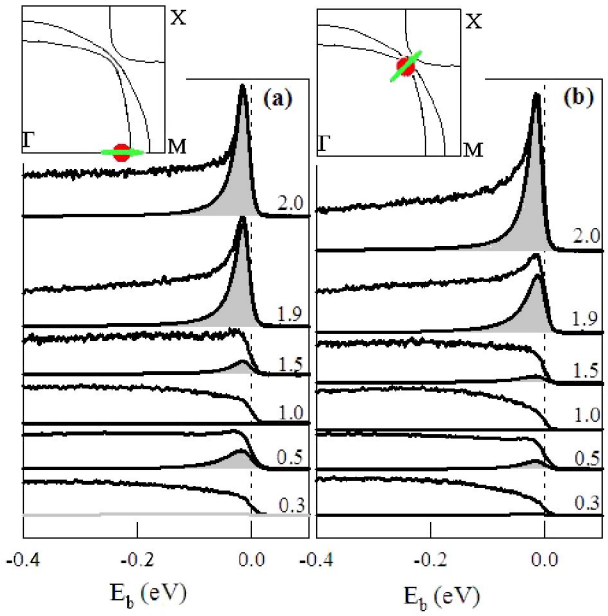

FIG. 4 (color online). ARPES EDCs of $Ca_{2-x}Sr_xRuO_4$ with $x = 0.3$, 0.5, 1.0, 1.5, 1.9, and 2.0, taken at the sample temperature of 20–40 K and the k_F of the β FS along (a) Γ-M and (b) Γ-X directions shown in the inset where the solid lines are the calculated FS of Sr_2RuO_4 [34]. The QP spectral weight is represented in the shadow area for different doping levels.

spectral weight observed indicates that the effect of Mott localization instead of disorder is dominant. For $x < 0.2$, the system becomes an antiferromagnetic Mott insulator, whose QP spectral weight at E_F completely diminishes (not shown).

To quantify the doping dependence of the QP line shape from the ARPES spectra for $x \geq x_c$, we extract the QP spectral weight (Z_{QP}) by fitting an ARPES spectrum with a broad incoherent background and a sharp coherent peak, and then modified by the Fermi function [30,31]. The value of Z_{QP} is obtained through normalized energy integral from the coherent peak. The fitting results along both the Γ-M and Γ-X directions are presented in Fig. 3(b). For better comparison with other results shown in Fig. 3(a), we plot the inverse ratio of Z_{QP} to the total spectral weight Z_{all}, i.e., Z_{all}/Z_{QP}. Again, Z_{all}/Z_{QP} also follow the Nordheim rule, indicating that the doping-induced random disorder directly accounts for the evolution of the QP spectral weight through the influence on the low-energy electron excitations.

In summary, we have studied the doping dependence of the local electronic properties of $Ca_{2-x}Sr_xRuO_4$ using LEED, STM, and ARPES. We found that, regardless of the fact of a well-ordered lattice structure, a local surface electronic inhomogeneity exists in the doped system as reflected by the nanoscale electronic corrugation. The doping dependence of such an electronic inhomogeneity, which follows the Nordheim rule in the same manner as that of the bulk in-plane residual resistivity, can be explained as a consequence of doping-induced random disorder. The intensity of the QP coherence peak in ARPES as a function of doping draws the same conclusion. These demonstrate that, for the first time, the doping-induced electronic inhomogeneity observed at the surface reflects the bulk property.

This work is supported by NSF DMR-0346826, DMR-0353108, DMR-0451163, DOE DE-FG02-04ER46125, DOE DMS, and ORAU faculty summer research program. The work at Oak Ridge National Laboratory (ORNL) is supported by BES of DOE. ORNL is managed by UT-Battle for US DOE under Contract No. DE-AC05-00OR22725. The Synchrotron Radiation Center was supported by NSF DMR-0084402.

[1] E. Dagotto, Science **309**, 257 (2005).
[2] J. Orenstein and A. J. Millis, Science **288**, 468 (2000).
[3] A. Moreo *et al.*, Science **283**, 2034 (1999).
[4] E. Miranda and V. Dobrosavljevic, Rep. Prog. Phys. **68**, 2337 (2005).
[5] P. Limelette *et al.*, Phys. Rev. Lett. **91**, 016401 (2003).
[6] T. Cren *et al.*, Phys. Rev. Lett. **84**, 147 (2000).
[7] S. H. Pan *et al.*, Nature (London) **413**, 282 (2001).
[8] C. Howald *et al.*, Phys. Rev. B **64**, 100504 (2001).
[9] Y. Kohsaka *et al.*, Phys. Rev. Lett. **93**, 097004 (2004).
[10] M. Uehara *et al.*, Nature (London) **399**, 560 (1999).
[11] M. Fäth *et al.*, Science **285**, 1540 (1999).
[12] K. McElroy *et al.*, Science **309**, 1048 (2005).
[13] T. J. Sato, J. W. Lynn, and B. Dabrowski, Phys. Rev. Lett. **93**, 267204 (2004).
[14] S. Nakatsuji and Y. Maeno, Phys. Rev. Lett. **84**, 2666 (2000); Phys. Rev. B **62**, 6458 (2000).
[15] O. Friedt *et al.*, Phys. Rev. B **63**, 174432 (2001).
[16] Y. Maeno *et al.*, Nature (London) **372**, 532 (1994).
[17] S. H. Pan *et al.*, Nature (London) **403**, 746 (2000).
[18] Ch. Renner *et al.*, Phys. Rev. Lett. **80**, 149 (1998).
[19] A. Yazdani *et al.*, Phys. Rev. Lett. **83**, 176 (1999).
[20] E. W. Hudson *et al.*, Science **285**, 88 (1999).
[21] J. E. Hoffman *et al.*, Science **295**, 466 (2002); **297**, 1148 (2002).
[22] T. Hanaguri *et al.*, Nature (London) **430**, 1001 (2004);
[23] Ch. Renner *et al.*, Nature (London) **416**, 518 (2002).
[24] Z.-X. Shen and D. S. Dessau, Phys. Rep. **253**, 1 (1995).
[25] A. Damascelli *et al.*, Rev. Mod. Phys. **75**, 473 (2003).
[26] R. Jin *et al.*, cond-mat/0112405.
[27] R. Matzdorf *et al.*, Science **289**, 746 (2000); Phys. Rev. B **65**, 085404 (2002).
[28] L. Nordheim, Ann. Phys. (Leipzig) **9**, 607 (1931).
[29] J. M. Ziman, *Electrons and Phonons* (Oxford, Clarendon, 1960), Vol. 337, p. 247.
[30] H. Ding *et al.*, Phys. Rev. Lett. **87**, 227001 (2001).
[31] D. L. Feng *et al.*, Science **289**, 277 (2000).
[32] A. Damascelli *et al.*, Phys. Rev. Lett. **85**, 5194 (2000).
[33] S.-C. Wang *et al.*, Phys. Rev. Lett. **93**, 177007 (2004).
[34] D. J. Singh, Phys. Rev. B **52**, 1358 (1995).